

SUPPORTING INFORMATION FOR

A DFT study on the direct benzene hydroxylation catalyzed by framework Fe and Al sites in zeolites

Gang Yang^{*a, b} and Lijun Zhou^a

^a College of Resources and Environment & Chongqing Key Laboratory of Soil Multi-scale Interfacial Process, Southwest University, 400715, Chongqing, China

^b Engineering Research Center of Forest Bio-preparation, Ministry of Education, Northeast Forestry University, Harbin 150040, China

S1. Computational methodologies

All calculations were carried out using Gaussian03 and Gaussian09 programs of suite^{1,2}. In accord with the previous work³, the H-form ZSM-5 zeolite was represented by 33-T cluster models (Fig. 1a), where the heteroatom (M = Fe, Al) occupies one of the T12 sites. The (OSiO)M(OHSiO)(OSiH₂) fragment of zeolites as well as adsorbent species were defined as the high-level region and calculated at the B3LYP/bs1 level of theory, whereas the rest were referred to the low-level region treated by B3LYP/3-21G method^{3,4}. In bs1, the 6-31+G(d,p) basis set was used for all elements except Fe that was described by the LANL2DZ effective core potential (ECP) basis set⁵. The iron-associated structures were considered at the sextet state (total spin = $5/2$) because of the lower energies than the corresponding quartet ones, which is in agreement with the previously reported results⁵⁻¹⁵. As shown in Fig. 1b, the three-coordinated Al and Fe sites in the framework (\mathbf{M}_L , M = Al, Fe) were constructed by removing one neighboring O atom from the corresponding H-form ZSM-5 zeolites¹⁶⁻¹⁹, and the same computational schemes as in the H-form zeolites were applied to the three-coordinated framework Al and Fe structures. In order to facilitate the understanding of the Lewis acidity of such Al and Fe species, the Wiberg bond indices that have been recognized as an effective method to measure bond strengths²⁰ were calculated by use of natural bond orbital (NBO) program²¹.

On basis of the optimized structures, the single-point energy calculations were performed with the two-layer ONIOM(M06L/bs2:B3LYP/6-31G(d)) scheme³. M06L^{22,23} is a recently developed meta-GGA (Generalized Gradient Approximation) functional that accounts for dispersive interactions. In bs2, the 6-311++G(d,p) basis set was chosen for all elements, while Fe as an exception was described by the LanL2TZ(f) ECP basis set²⁴.

References:

1. Gaussian 03, Revision A.02, Frisch, M.J.; Trucks, G.W.; Schlegel, H.B.; Scuseria, G.E.; Robb, M.A.; Cheeseman, J.R.; Montgomery, Jr., J.A.; Vreven, T.; Kudin, K.N.; Burant, J.C.; Millam, J.M.; Iyengar, S.S.; Tomasi, J.; Barone, V.; Mennucci, B.; Cossi, M.; Scalmani, G.; Rega, N.; Petersson, G.A.; Nakatsuji, H.; Hada, M.; Ehara, M.; Toyota, K.; Fukuda, R.; Hasegawa, J.; Ishida, M.; Nakajima, T.; Honda, Y.; Kitao, O.; Nakai, H.; Klene, M.; Li, X.; Knox, J.E.; Hratchian, H.P.; Cross, J.B.; Bakken, V.; Adamo, C.; Jaramillo, J.; Gomperts, R.; Stratmann, R.E.; Yazyev, O.; Austin, A.J.; Cammi, R.; Pomelli, C.; Ochterski, J.W.; Ayala, P.Y.; Morokuma, K.; Voth, G.A.;

- Salvador, P.; Dannenberg, J.J.; Zakrzewski, V.G.; Dapprich, S.; Daniels, A.D.; Strain, M.C.; Farkas, O.; Malick, D.K.; Rabuck, A.D.; Raghavachari, K.; Foresman, J.B.; Ortiz, J.V.; Cui, Q.; Baboul, A.G.; Clifford, S.; Cioslowski, J.; Stefanov, B.B.; Liu, G.; Liashenko, A.; Piskorz, P.; Komaromi, I.; Martin, R.L.; Fox, D.J.; Keith, T.; Al-Laham, M.A.; Peng, C.Y.; Nanayakkara, A.; Challacombe, M.; Gill, P.M.W.; Johnson, B.; Chen, W.; Wong, M.W.; Gonzalez, C.; Pople, J.A.; Gaussian, Inc., Wallingford CT, **2004**.
2. Gaussian 09, Revision A.9, Frisch, M.J.; Trucks, G.W.; Schlegel, H.B.; Scuseria, G.E.; Robb, M.A.; Cheeseman, J.R.; Scalmani, G.; Barone, V.; Mennucci, B.; Petersson, G.A.; Nakatsuji, H.; Caricato, M.; Li, X.; Hratchian, H.P.; Izmaylov, A.F.; Bloino, J.; Zheng, G.; Sonnenberg, J.L.; Hada, M.; Ehara, M.; Toyota, K.; Fukuda, R.; Hasegawa, J.; Ishida, M.; Nakajima, T.; Honda, Y.; Kitao, O.; Nakai, H.; Vreven, T.; Montgomery, Jr., J.A.; Peralta, J.E.; Ogliaro, F.; Bearpark, M.; Heyd, J.J.; Brothers, E.; Kudin, K.N.; Staroverov, V.N.; Kobayashi, R.; Normand, J.; Raghavachari, K.; Rendell, A.; Burant, J.C.; Iyengar, S.S.; Tomasi, J.; Cossi, M.; Rega, N.; Millam, N.J.; Klene, M.; Knox, J.E.; Cross, J.B.; Bakken, V.; Adamo, C.; Jaramillo, J.; Gomperts, R.; Stratmann, R.E.; Yazyev, O.; Austin, A.J.; Cammi, R.; Pomelli, C.; Ochterski, J.W.; Martin, R.L.; Morokuma, K.; Zakrzewski, V.G.; Voth, G.A.; Salvador, P.; Dannenberg, J.J.; Dapprich, S.; Daniels, A.D.; Farkas, Ö.; Foresman, J.B.; Ortiz, J.V.; Cioslowski, J.; Fox, D.J. Gaussian, Inc., Wallingford CT, **2009**.
3. Yang, Z. W.; Yang, G.; Liu, X. C.; Han, X. W. *Catal. Lett.* **2013**, *143*, 260-266.
4. Yang, G.; Zhou, L. J.; Liu, X. C.; Han, X. W.; Bao, X. H. *Chem. Eur. J.* **2011**, *17*, 1614-1621.
5. Hay, P. J.; Wadt, W. R. *J. Chem. Phys.* **1985**, *82*, 299-310.
6. Yakovlev, A. L.; Zhidomirov, G. M.; van Santen, R. A. *J. Phys. Chem. B* **2001**, *105*, 12297-12302.
7. Ryder, J. A.; Chakraborty, A. K.; Bell, A. T. *J. Catal.* **2003**, *220*, 84-91.
8. Pantu, P.; Pabchanda, S.; Limtrakul, J. *ChemPhysChem* **2004**, *5*, 1901-1906.
9. Shiota, Y.; Suzuki, K.; Yoshizawa, K. *Organometallics* **2006**, *25*, 3118-3123.
10. Yang, G.; Zhou, L. J.; Liu, X. C.; Han, X. W.; Bao, X. H. *J. Phys. Chem. B* **2006**, *110*, 22295-22297.
11. Fellah, M. F.; van Santen, R. A.; Onal, I. *J. Phys. Chem. C* **2009**, *113*, 15307-15313.
12. Yang, G.; Zhou, L. J.; Liu, X. C.; Han, X. W.; Bao, X. H. *J. Phys. Chem. C* **2009**, *113*, 18184-18190.
13. Fellah, M. F.; Onal, I.; van Santen, R. A. *J. Phys. Chem. C* **2010**, *114*, 12580-12589.
14. Rosa, A.; Ricciardi, G.; Baerends, E. J. *Inorg. Chem.* **2010**, *49*, 3866-3880.
15. Li, G. N.; Pidko, E. A.; van Santen, R. A.; Feng, Z. C.; Li, C.; Hensen, E. J. M. *J. Catal.* **2011**, *284*, 194-206.
16. van Bokhoven, J. A.; van der Eerden, A. M. J.; Koningsberger, D. K. *J. Am. Chem. Soc.* **2003**, *125*, 7435-7442.
17. Wischert, R.; Copéret, C.; Delbecq, F.; Sautet, P. *Chem. Comm.* **2011**, *47*, 4890-4892.

18. Wischert, R.; Laurent, P.; Copéret, C.; Delbecq, F.; Sautet, P. *J. Am. Chem. Soc.* **2012**, *134*, 14430-14449.
19. Sokol, A. A.; Catlow, R. A.; Garcés, J. M.; Kuperman, A. *Adv. Mater.* **2000**, *12*, 1801-1805.
20. Wiberg, K. B. *Tetrahedron* **1968**, *24*, 1083-1096.
21. Glendening, E. D.; Reed, A. E.; Carpenter, J. E.; Weinhold, F. *NBO version 3.1*.
22. Zhao, Y.; Truhlar, D. G. *J. Chem. Phys.* **2006**, *125*, 194101.
23. Zhao, Y.; Truhlar, D. G. *Theor. Chem. Acc.* **2008**, *120*, 215-241.
24. Roy, L. E.; Hay, P. J.; Martin, R. L. *J. Chem. Theory Comput.* **2008**, *4*, 1029-1031.

S2. Configuration distortions of the Brønsted (M_B) and Lewis (M_L) acidic sites ($M = Al, Fe$)

For the framework Lewis acidic sites (Fig. 1b), the deviation degree of the metal centers ($M = Al, Fe$) from the O₁O₂O₃ plane can be characterized by the parameter Λ_M defined as¹,

$$\Lambda_M = \text{average} [\phi(O_1O_3O_2M), \phi(O_3O_2O_1M), \phi(O_2O_1O_3M)] \quad (1)$$

The Λ_{Al} value is calculated to be 11.71° (Table S1) and accordingly, the Al center of the framework Lewis acidic site (Al_L) adopts a configuration that distorts somewhat from the experimentally postulated planar triangle², probably due to the strain force enforced by the associated zeolite framework. In the Al(OH)₃ molecule with no extraneous strain force (Fig. S1), each of the $\phi(O_1O_3O_2Al)$, $\phi(O_3O_2O_1Al)$, $\phi(O_2O_1O_3Al)$ dihedrals is optimized to equal exactly 0°, indicating the perfectly planar triangle. This corroborates that the configurational distortion of Al_L is caused by the associated zeolite framework. As shown in Table 1, the framework Fe-O bond lengths in zeolites are even larger [3-5], and a more significantly strain force is assumed. As a result, a larger configurational distortion is predicted for the Fe_L center, which is consistent with the calculated Λ_{Fe} value at 34.55°.

References:

1. Yang, G.; Pidko, E. A.; Hensen, E. J. M. *J. Phys. Chem. C* **2013**, *117*, 3976-3986.
2. van Bokhoven, J.A.; van der Eerden, A.M.J.; Koningsberger, D.K. *J. Am. Chem. Soc.* **2003**, *125*, 7435-7442.
3. Chatterjee, A.; Iwasaki, T.; Ebina, T.; Miyamoto, A. *Micropor. Mesopor. Mater.* **1998**, *21*, 421-428.
4. Yuan, S. P.; Wang, J. G.; Li, Y. W.; Jiao, H. J. *J. Phys. Chem. A* **2002**, *106*, 8167-8172.
5. Wang, Y.; Yang, G.; Zhou, D. H.; Liu, X. C.; Bao, X. H. *J. Phys. Chem. B* **2004**, *108*, 18228-18233.

Table S1. The average M-O bond distances (r , in Å) in the Brønsted ($\mathbf{M_B}$) and Lewis ($\mathbf{M_L}$) acidic sites of [M]-ZSM-5 zeolites as well as the deviation degrees of M centers from the O₁O₂O₃ planes (Λ , in degrees) in their Lewis ($\mathbf{M_L}$) acidic sites (M = Al, Fe)

	Lewis ($\mathbf{M_L}$)			Brønsted ($\mathbf{M_B}$)		
	Al-O	Λ_{Al}	Fe-O	Λ_{Fe}	Al-O	Fe-O
B3LYP/bs1:B3LYP/3-21G	1.665	11.71	1.765	34.55	1.717	1.805
Experimental ^a		planar			1.65~1.75	

^a *J. Am. Chem. Soc.* **2003**, *125*, 7435-7442.

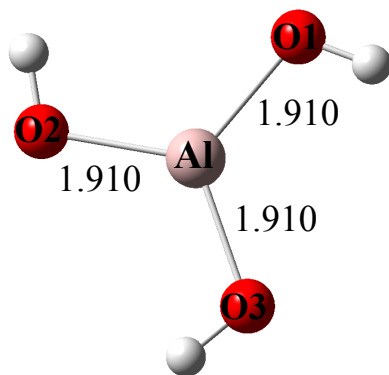


Fig. S1. Optimized structure of Al(OH)₃. Selected distances are given in Å.

S3. O₃ decomposition

Besides N₂O, O₃ has also been used for generation of the α -oxygen species that shows catalysis for the benzene hydroxylation reaction. As shown in Fig. S2, the reaction mechanism of O₃ decomposition resembles that of N₂O decomposition discussed in the text. The ONIOM(B3LYP/bs2:B3LYP/6-31G*) energy calculations give a neglectable energy barrier of 0.7 kcal mol⁻¹. This is in agreement with the single-point energy results at the ONIOM(M06L/bs2:B3LYP/6-31G*) level (-1.7 kcal mol⁻¹).

The calculated $\langle S_2 \rangle$ values are given in Table S2, which are very close to the expected values. It thus indicates that the spin contaminations can be neglected in our calculations.

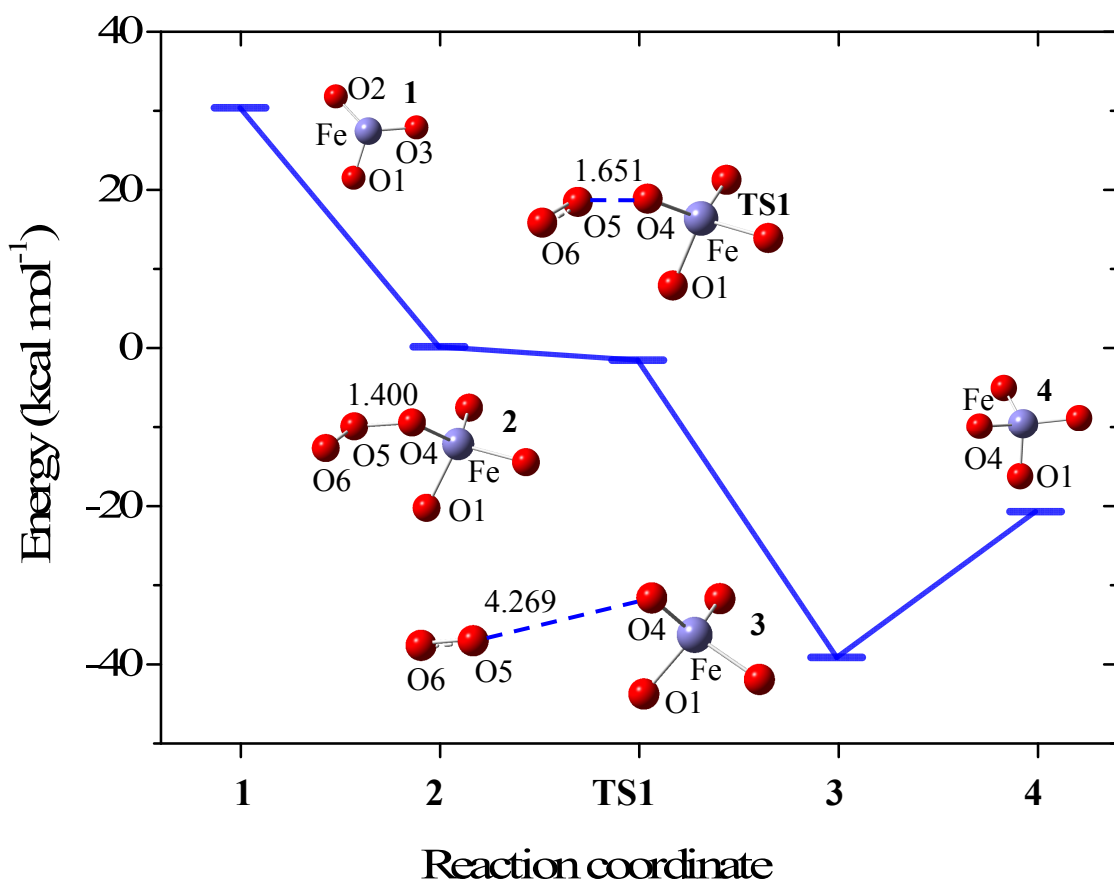


Fig. S2. The ONIOM(M06L:B3LYP) energy diagram of O₃ decomposition over the Fe Lewis acidic site of [Fe]-ZSM-5 zeolite as well as the local structures of energy minima and transition states. Selected distances are given in Å.

Table S2. The spin densities and $\langle S^2 \rangle$ values for structures of O₃ decomposition over framework Fe Lewis acidic site of [Fe]-ZSM-5 zeolite^a

	1	2	TS1	3	4
s(Fe)	4.182	3.728	3.408	2.567	3.224
Expected $\langle S^2 \rangle$	8.750	8.750	8.750	8.750	8.750
Calculated $\langle S^2 \rangle$	8.750	8.751	8.756	8.752	8.750

^a Calculated at the ONIOM(M06L:B3LYP)//B3LYP level.

S4. Stability of the α -oxygen species

As demonstrated in the text, N₂O decomposition on framework Fe Lewis acidic site (**Fe_L**, **1**) results in the formation of the α -oxygen species (**4**, Fig. 4b). Different from the case of framework Al Lewis acidic site (Fig. 4a), the α -oxygen species of framework Fe Lewis acidic site is self-stable and can induce chemical reactions such as the presently investigated benzene hydroxylation.

The stability of the α -oxygen species (ΔE_1) corresponding to framework Fe Lewis acidic site is evaluated by,

$$(\Delta E_1) = E(\mathbf{4}) - E(\mathbf{1}) - E(\text{O}) \quad (1)$$

where $E(\mathbf{4})$ and $E(\mathbf{1})$ are respectively the energies of structures **4** and **1**, while $E(\text{O})$ represents the energy of the oxygen atom (O).

As to the extra-lattice Fe site [1], the stability of the α -oxygen species (ΔE_2) can also be obtained in the same way. Then the stability difference of the α -oxygen species between framework and extra-framework Fe sites is written as,

$$\Delta\Delta E = \Delta E_1 - \Delta E_2 \quad (2)$$

The $\Delta\Delta E$ value is calculated to be 13.5 kcal mol⁻¹. Accordingly, the α -oxygen species of framework Fe Lewis acidic site is less stable and hence should be more catalytically active. This explains why the adsorption of benzene on the α -oxygen species of framework Fe Lewis acidic site results in the direct formation of O4-C1 bond and zeolites with framework Fe sites show superior catalysis for the benzene hydroxylation reaction [2-6].

References:

1. Yang, Z. W.; Yang, G.; Liu, X. C.; Han, X. W. *Catal. Lett.* 2013, **143**, 260-266.
2. Chang, Y. F.; McCarty, J. G.; Zhang, Y. L. *Catal. Lett.* 1995, **34**, 163-177.
3. Ribera, A.; Arends, I. W. C. E.; de Vries, S.; Pérez-Ramírez, J.; Sheldon, R. A. *J. Catal.* 2000, **195**, 287-297.
4. Meloni, D.; Monaci, R.; Solinas, V.; Berlier, G.; Bordiga, S.; Rossetti, I.; Oliva, C.; Forni, L. *J. Catal.* 2003, **214**, 169-178.
5. Yuranov, I.; Bulushev, D. A.; Renken, A.; Kiwi-Minsker, L. *J. Catal.* 2004, **227**, 138-147.
6. Lee, J. K.; Kim Y. J.; Lee, H. J.; Kim, S. H.; Cho, S. J.; Nam, I. S.; Hong, S. B. *J. Catal.* 2011, **284**, 23-33.

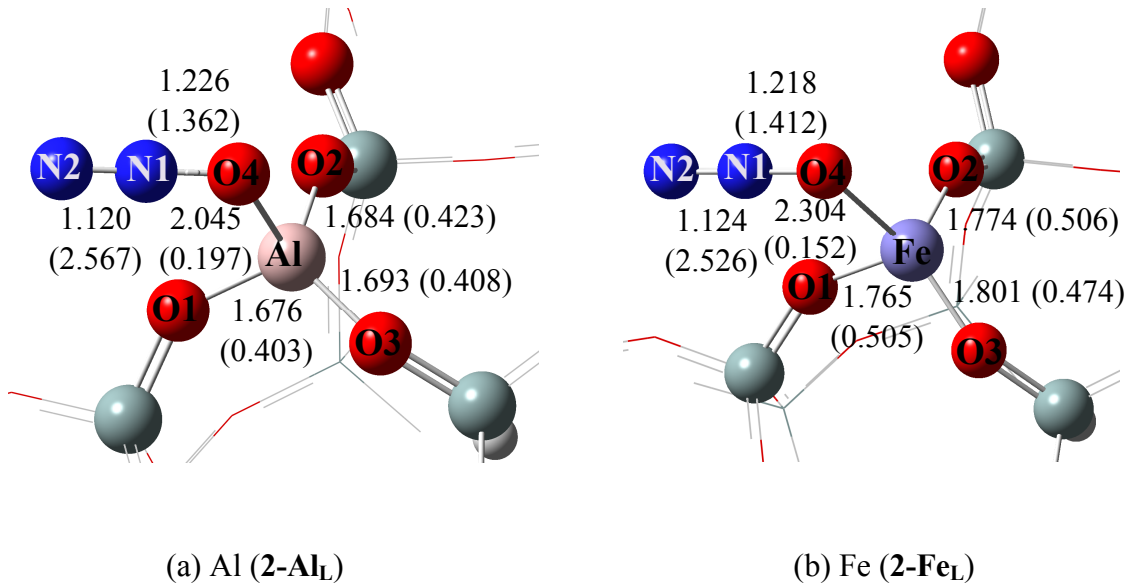


Fig. S3. The local structures of N₂O adsorption on the Lewis acidic sites of [Al]- and [Fe]-ZSM-5 zeolites. Selected bond lengths are given in Å, and their bond orders are also shown (in parentheses).

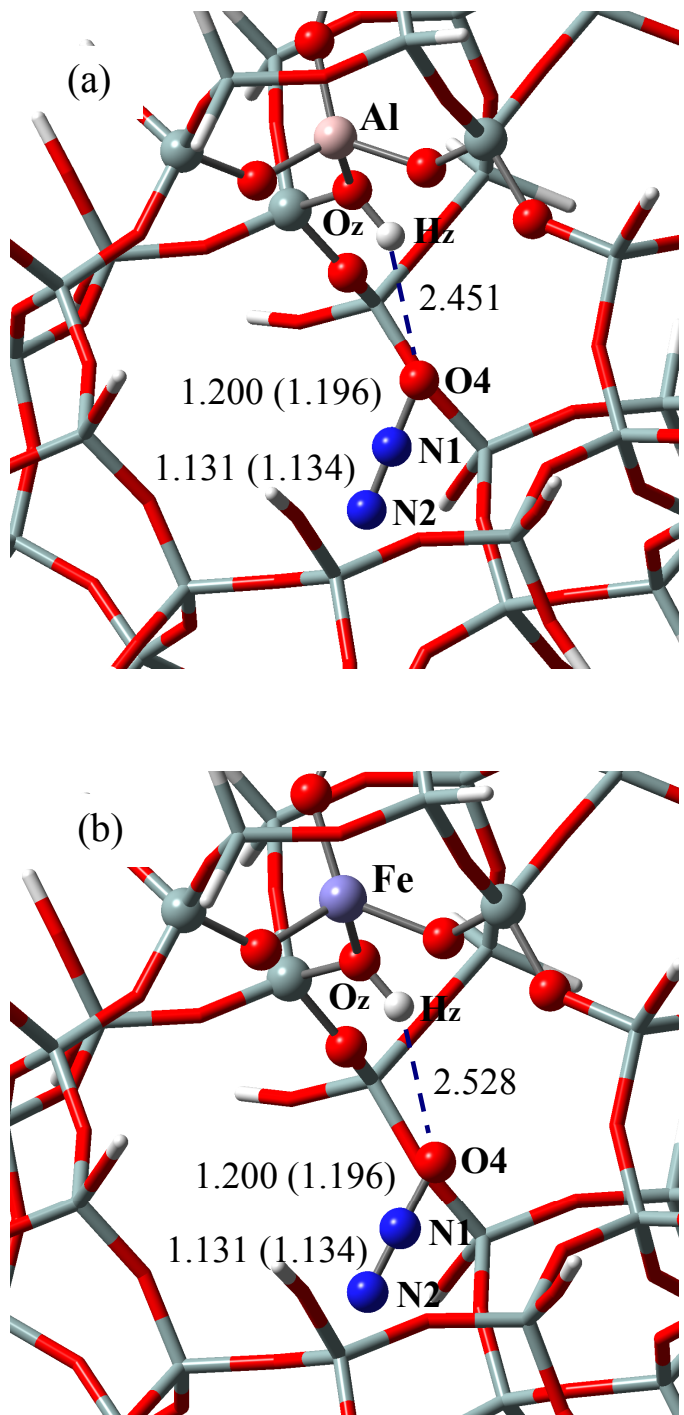


Fig. S4. Structures of N_2O adsorption on the Brønsted acidic sites ($\mathbf{M_B}$) of $[\mathbf{M}]\text{-ZSM-5}$ zeolites ($\mathbf{X = Al, Fe}$). Selected distances are given in Å, and the bond distances of gas-phase N_2O are shown in parentheses.

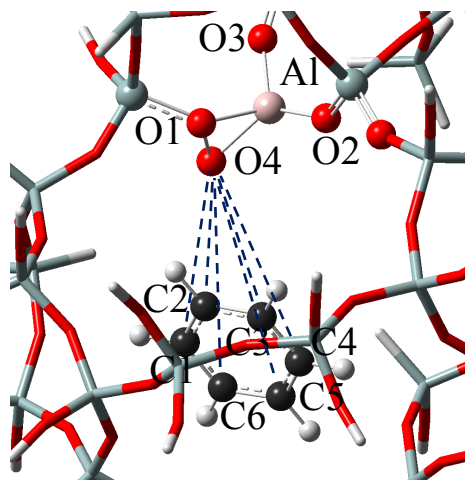


Fig. S5. The adsorption configuration of benzene on the α -oxygen site of the framework Al Lewis acidic site of [Al]-ZSM-5 zeolite.